MODELLING OF FLUID-PHASE ENDOCYTOSIS KINETICS IN THE AMOEBAE OF THE CELLULAR SLIME MOULD *DICTYOSTELIUM DISCOIDEUM*. A MULTICOMPARTMENTAL APPROACH.

Laurence Aubry[‡], Gérard Klein[‡], Jean-Louis Martiel[¶] and Michel Satre[‡]

[‡]Laboratoire de Biologie Cellulaire, URA 1130 CNRS, CEA, Département de Biologie Moléculaire et Structurale, Centre d'Etudes Nucléaires, 17, rue des Martyrs, 38054 Grenoble Cedex 9, France.
[¶]Laboratoire de Techniques d'Imagerie, de Modélisation et de Cognition (TIMC), URA 1618 CNRS, Département de Mathématiques, Faculté de Médecine, 38700 La Tronche, France.

ABSTRACT

Fluid-phase endocytosis (pinocytosis) kinetics were studied in *Dictyostelium discoideum* amoebae from the axenic strain Ax-2 that exhibits high rates of fluid-phase endocytosis when cultured in liquid nutrient media. Fluorescein-labelled dextran (FITC-dextran) was used as a marker in continuous uptake- and in pulse-chase exocytosis experiments. In the latter case, efflux of the marker was monitored on cells loaded for short periods of time and resuspended in marker-free medium. A multicompartmental model was developed which describes satisfactorily fluid-phase endocytosis kinetics. In particular, it accounts correctly for the extended latency period before exocytosis in pulse-chase experiments and it suggests the existence of some sorts of maturation stages in the pathway.

1. INTRODUCTION

Endocytosis is the biological process whereby extracellular material is transported inside the cell by means of plasma membrane derived vesicles and it comprises phagocytosis, receptor-mediated endocytosis and fluid-phase endocytosis (Besterman & Low, 1983; Steinman *et al*, 1983). It plays a key role in the physiology of most eucaryotes and is involved in diverse activities such as entry of nutriments and essential elements,

Acta Biotheoretica **43**: 319–333, 1995.

maintenance of plasma membrane composition, response to hormones and growth factors, ingestion of inert particles, viruses and bacteria (Smythe & Warren, 1991; Sorkin & Waters, 1993; Watts & Marsh, 1992).

Fluid-phase endocytosis or pinocytosis is the bulk uptake of soluble (non-particulate) extracellular components. Fluid entry occurs concurrently with receptor-mediated endocytosis in clathrin-coated vesicles (Keen, 1990) but may proceed independently of the receptor-mediated pathway (Sandvig & Van Deurs, 1991; Van Deurs *et al*, 1989). Fluid-phase endocytosis is usually considered to be a constitutive process although it is influenced by various physiologic conditions. It stops during mitosis (Berlin & Oliver, 1980; Berlin *et al*, 1978; Quintart *et al*, 1979) and is enhanced when cells are stimulated by growth factors or compounds such as phorbol esters (Swanson *et al*, 1985).

Internalised endocytic cargo passes through a series of complex vesicular structures morphologically and biochemically defined. Although there is at present no standard nomenclature for the different compartments encountered along the endocytic pathway (Courtoy, 1991), distinct classes of vesicular compartments are distinguished within the context of either a vesicular shuttle or a maturation hypothesis (Griffiths & Gruenberg, 1991; Murphy, 1991). At the earliest times, clathrin-coated vesicles are formed from coated pits at the cell surface. They rapidly uncoat to form smooth vesicles or primary endocytic vesicles of small size with a diameter of about 0.1 μm (Swanson *et al*, 1981). They are endowed with the capacity to fuse with one another through homotypic fusion to form early endosomes (Griffiths & Gruenberg, 1991; Helenius *et al*, 1983). These structures are also named CURL (i.e. compartment of uncoupling receptor and ligand) or sorting endosomes. Most solutes are further transported in maturing endosomes or multivesicular bodies while in higher eucaryotes recycling vesicles (or tubulo-vesicles) return most of the receptors and membrane from the early endosomal compartment to the plasma membrane. The next compartments are late endosomes or prelysosomes and these multivesicular structures are thought to be the sites where (1) lysosomal enzymes are delivered from the trans Golgi reticulum to the endocytic pathway and (2) solutes start to be transported to the cytosol if appropriate membrane carriers are available. The following secondary lysosomes are the most efficient sites for digestion of ingested material. They are not dead-end cellular spaces as they remain active in term of membrane traffic. In *Dictyostelium*, postlysosomal vesicles return both membrane and "indifferent" solutes to the plasma membrane (Aubry *et al*, 1993; Padh *et al*, 1993).

Amoebae of the cellular slime mould *Dictyostelium discoideum* depend on endocytosis as their single way of food uptake. In the laboratory, wild type strains phagocytose avidly enterobacteria such as *Escherichia coli* or *Klebsiella aerogenes* and divide every 3 hours. Strains Ax-2 and Ax-3 derived from wild-type NC-4 have been specifically selected for growth in liquid nutrient medium (Loomis, 1971; Watts & Ashworth, 1970). They bear mutations *axe*A and *axe*B that map to linkage groups II and III, allowing axenic strains to double every 8-10 hours in the absence of any solid food source. Axenic strains of *Dictyostelium discoideum* are remarkably well suited to study fluid-phase endocytosis as they show a strongly enhanced capacity as compared to the wild-type NC-4 (Clarke & Kayman, 1987; Maeda, 1983). It seems plausible that rapid fluid-phase endocytosis is required for axenic growth. Fluid entry occurs mainly via the clathrin-coated vesicles pathway as *Dictyostelium* cells constructed to be deficient in clathrin heavy chain synthesis are severely affected in fluid-phase endocytosis (O'Halloran & Anderson, 1992; Ruscetti *et al*, 1994).

Quantitative data generated in experimental studies of fluid-phase endocytosis are most often analysed without mathematical modelling. In principle, data analysis using kinetic models could permit rigorous description of the process and could furthermore be used in simulation studies to generate quantitative predictions of endocytic behaviour. In cells such as hepatocytes, mathematical models have been successfully developed (Blomhoff *et al*, 1989; Scharschmidt *et al*, 1986). The basic theory of such models is given in the literature (Atkins, 1973; DiStefano & Landaw, 1984; Landaw & DiStefano, 1984). In this paper, a linear compartmental analytic approach has been employed to construct a kinetic model of fluid-phase endocytosis in *Dictyostelium* amoebae. This model was then used to analyse data from both pulse-chase and continuous incubation experiments with FITC-dextran as a fluid-phase marker.

2. MATERIAL AND METHODS

2.1. Culture Conditions

Dictyostelium discoideum Ax-2 amoebae (American Type Culture Collection #24937, Rockville, Maryland, USA) were grown at 21°C with rotary agitation at 170 rpm in peptone-yeast extract medium, pH 6.5, containing 18 g/l maltose and 0.25 g/l dihydrostreptomycin (Watts & Ashworth, 1970). Amoebae were always collected in their logarithmic phase of growth (4×10^6 to 1×10^7 cells/ml).

2.2. Fluid-Phase Endocytosis Measurements

Fluid-phase endocytosis measurements in *Dictyostelium* amoebae were routinely conducted with FITC-dextran as a fluid-phase marker (Aubry *et al*, 1993; Klein & Satre, 1986; Padh *et al*, 1993). Briefly, amoebae (5×10^6/ml) were incubated at 21°C in growth medium containing 4 mg/ml FITC-dextran either continuously or for various pulse periods (see legends to figures for specific conditions). Cells were then washed twice in ice-cold 20 mM Mes-Na buffer, pH 6.5, 0.05% (w/v) bovine serum albumin (Mes buffer) and resuspended at 5×10^6 amoebae/ml in growth medium at 21°C. This washing step was omitted for continuous loading conditions. Aliquots (1 ml) of the cell suspension were taken as a function of time, washed twice in ice-cold Mes buffer as described above, resuspended in 1 ml Mes buffer and counted with a Coulter ZM counter. To measure the amount of internalised FITC-dextran, amoebae were lysed by a further addition of 2 ml 100 mM Na_2HPO_4-0.25% (v/v) Triton X-100 and the fluorescence intensity was measured at excitation and emission wavelengths of 470 and 520 nm, respectively. When 8-hydroxypyrene-1,3,6-trisulfonic acid (pyranine) was used simultaneously as a second fluid-phase marker, another aliquot sample of amoebae was lysed in 100 mM NaH_2PO_4-0.25% (v/v) Triton X-100 and the fluorescence intensity was measured at excitation and emission wavelengths of 410 and 520 nm, respectively. In these acidic conditions, fluorescence contribution of fluorescein was negligible. By comparison to a FITC-dextran or pyranine calibration curve, fluorescence data were converted either in an amount of fluid-phase marker: $Q(t)$ in fg/cell or in an equivalent volume of internalised fluid (endocytic index): $U(t)$, by taking into account the marker concentration C (fg/fl) in the incubation medium. As the cell volume (Klein & Satre, 1986) is less than 0.5% of the total incubation volume, C can be considered to be constant during continuous loading and

negligible during chase experiments. In *Dictyostelium* amoebae as well as in other eucaryotes, a marked concentration of solutes occurs during the intracellular transit of endocytic vesicles (Thilo, 1985). Care must be taken when comparing endocytic volume flow data with actual volumes involved. Volumes of endocytic compartments discussed in this work are thus only apparent volumes and will not usually match their anatomical counterparts (see under "Results and Discussion").

FITC-dextran (Mr = 70 000) was synthesised in the laboratory by reacting dextran (dextran T70, Pharmacia) with fluorescein isothiocyanate (De Belder & Granath, 1973). Pyranine was purchased from Lancaster, England.

2.3. Multicompartmental Model and Equations

Compartmental modelling of the fluid-phase endocytic system consists in representing the process by a set of compartments interacting with each other through the transfer of internalised fluid as reported by the fluid-phase marker (Fig. 1). During a full endocytic cycle starting from the entry of the marker at time zero in the cell until its exit, compartments are defined by their position on a time scale along the pathway. They are characterised by their apparent volumes and by the rates of transfer. It is assumed that transfer processes follow simple first-order kinetics so that rates are directly proportional to the amount of material available for transfer. In the pulse-chase or continuous load experiments, the intracellular pathway is always saturated either by marked fluid or by the regular feeding solution. This condition allows us to use linear models for the dynamics of the intracellular endocytic traffic.

Let us denote by $U_i(t)$ the amount of marked fluid (in fl/cell) in the compartment i at time t. The temporal evolution of the compartment content may be expressed in the following form:

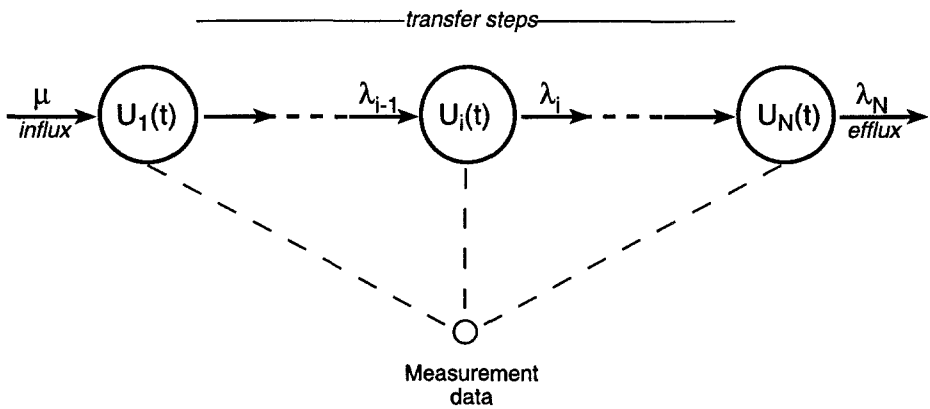

Fig. 1. Multicompartmental model for fluid-phase endocytosis in *Dictyostelium discoideum* amoebae. FITC-dextran marker is transferred from the external medium to the endo-lysosomal compartments and ultimately back to the medium. The various λ_i and U_i are the rate constants (min^{-1}) and the amount of marked fluid (fl/cell), respectively and μ is the input rate of fluid in the cell (fl/cell/min). Measurement data represent intracellular FITC-dextran.

$$\begin{aligned} \frac{dU_1(t)}{dt} &= \mu(t) - \lambda_1 U_1(t) \\ \frac{dU_i(t)}{dt} &= \lambda_{i-1} U_{i-1}(t) - \lambda_i U_i(t) \\ \frac{dU_N(t)}{dt} &= \lambda_{N-1} U_{N-1}(t) - \lambda_N U_N(t) \end{aligned} \tag{1}$$

In the above system of coupled linear differential equations, $\mu(t)$ is the input rate of external fluid in the cell (in fl/cell/min) and is associated with the first compartment (Fig. 1); the coefficient λ_i (in min^{-1}) is the transfer rate from compartment (i) to (i+1). Recycling to the extracellular medium is assumed to occur after the last compartment only with a rate constant denoted λ_N. Initial conditions were fixed at:

$$U_i(t=0) = 0 \text{ for } i = 1, \ldots, N \tag{2}$$

The time function $\mu(t)$ is given by the expression:

$$\mu(t) = \begin{cases} \mu & \text{if} \quad 0 \le t \le T \\ 0 & \text{otherwise} \end{cases}$$

for a pulse-chase experiment of duration T and by: $\mu(t) = \mu \quad 0 \le t$ for continuous loading.

We will use this model to determine the numerical values of the unknown parameters, namely, the influx rate μ, the number of compartments N and the transfer rate λ_i from one compartment to its follower. At our disposal, we have the pulse duration (T) and the total amount of marked intracellular fluid at time t, which is denoted by $y(t_j)$, $j = 1, \ldots, np$. Instead of using directly the variable y, we normalise it by its maximum value available in the data series; the normalised variable is denoted z. The model prediction for the variable z, denoted $S(t,\mu)$, corresponds to the summation of the compartments content from 1 to N:

$$S(t,\mu) = \sum_{i=1}^{N} U_i(t,\mu)$$

Because of the linearity of the differential system (1), the solution vector U as well as the variable S are directly proportional to the parameter μ. We define the error function as the weighted sum of the squared differences between the values $z(t_j)$ and the model prediction:

$$\varepsilon = \sum_{j=1}^{np} w_j \left(z(t_j) - \mu S(t_j,1)\right)^2 \tag{3}$$

where w_j is the weight associated with the observation $z(t_j)$ taken as the reciprocal of the estimated variance associated to the observation $z(t_j)$. $S(t,1)$ is obtained from a solution of (1) with μ arbitrarily set to 1. The actual value of μ, used in the definition of ε, is given by the condition $\partial\varepsilon/\partial\mu = 0$, which reads:

$$\mu = \frac{\sum_{j=1}^{np} S(t_j,1) z(t_j) w_j}{\sum_{j=1}^{np} S(t_j,1)^2 w_j}$$

We determine the unknown parameters λ_j, $j = 1,...,N$ and N by solving the minimisation problem:

$$\min_{N = 1,2,...} \left[\min_{\substack{\lambda_j;\lambda_j > 0 \\ j = 1,...,N}} \{\varepsilon\} \right] \tag{4}$$

If we use more than one data set to fit the parameters, the definition of ε is slightly changed as:

$$\varepsilon = \frac{1}{N_{exp}} \sum_{k=1}^{N_{exp}} \sum_{j=1}^{np_k} w_{k,j}\left(z_k(t_j) - \mu_k S_k(t_j,1)\right)^2 \tag{5}$$

where N_{exp} is the number of experimental series used for parameter estimation. From the condition $\partial\varepsilon/\partial\mu_k = 0$ we get the expression for parameter μ_k:

$$\mu_k = \frac{\sum_{j=1}^{np} S_k(t_j,1) z_k(t_j) w_{k,j}}{\sum_{j=1}^{np} S_k(t_j,1)^2 w_{k,j}} \tag{6}$$

During the minimisation procedure we need to solve the differential system (1) (with the initial conditions (2) and an input set to 1). Since the system (1) is linear, we may use an implicit second order (Crank-Nicholson) method, which reads:

$$U^{n+1} - U^n = \frac{\Delta t}{2}\left(v^{n+1} + v^n\right) + \frac{\Delta t}{2}\left(KU^{n+1} + KU^n\right)$$

where Δt is the time step, U^n is the vector $(U_1(n\Delta t),...,U_N(n\Delta t))^t$; v^n is the vector $(\mu(n\Delta t),0,...,0)^t$; K is a band matrix whose main diagonal is $(-\lambda_1,-\lambda_2,...,-\lambda_N)$ and with a sub diagonal: $(\lambda_1,\lambda_2,...,\lambda_{N-1})$. From above, we get the approximation of U at time $(n+1)\Delta t$ as a linear function of U^n:

$$U^{n+1} = \frac{\Delta t}{2}\left(I - \frac{\Delta t}{2}K\right)^{-1}\left(v^{n+1} + v^n\right) + \left(I - \frac{\Delta t}{2}K\right)^{-1}\left(I + \frac{\Delta t}{2}K\right)U^n$$

where I is the identity matrix. This relation provides a numerical solution of (1) whose global error on a finite interval $(0,t_{max})$ remains proportional to Δt^2. The procedure is achieved by a direct search of the minimum of (4) using the routine BCPOL from the International Mathematical and Statistical Library (IMSL, Visual Numerics, Inc., Houston, USA) package (IMSL, 1991). BCPOL uses the complex method to find a minimum point of a function of n variables. The method is based on function comparison and no smoothness of the error function is assumed. The program starts with a complex consisting of $2n$ points $(x_1,..,x_i,...x_{2n})$ in the n-dimensional parameter space. At each iteration a new point is generated to replace the worst point in the former set of the complex. In addition, the program allows the use of simple bounds for the parameter. In our case, we restricted the lambda's to positive values only which is a natural boundary value. Computations were performed on a ALPHA/OSF2 DEC-Equipment station.

In a first step, we fix $N \geq 3$ and then we determine a set of λ_j minimizing ε. In these conditions, because we estimate the values of the μ's according to relation (6), the number

of degrees of freedom is defined as:

$$df(N) = \sum_{k=1}^{N_{exp}} np_k - N - N_{exp} \quad (7)$$

There are several ways to optimally estimate the model complexity parameter N. The simplest one is to consider the value of the error $\varepsilon(N)$ as a function of N; the optimal N_{opt} would give a minimum for ε. We may complicate our choice of N_{opt} by looking at the error per degree of freedom, i.e. the function $\varepsilon(N)/df(N)$. Finally, if we consider two models $M1$ and $M2$, characterised by $N1$ and $N2$ ($N1<N2$), $M1$ may be seen as a submodel of $M2$. If we assume that $M1$ is the 'exact' model, any subsequent increase of the number of free adjustable parameters would not result in a substantial drop for the error function. To check whether the improvement of the fit is significantly better than it would be by chance alone, we compute the F statistics (Landaw & DiStefano, 1984):

$$F = \frac{\left(\varepsilon(N_1) - \varepsilon(N_2)\right) / (N_2 - N_1)}{\varepsilon(N_2) / df(N_2)} \quad (8)$$

If we assume that the residuals are normally distributed, F is given by the Fischer distribution $F(N_2-N_1, df(N_2))$.

3. RESULTS AND DISCUSSION

3.1. Fluid-Phase Endocytosis Kinetics in *Dictyostelium discoideum* Amoebae

3.1.1 Continuous Loading

In this work, FITC-dextran was chosen as a fluid-phase marker to measure fluid-phase endocytosis in *Dictyostelium* amoebae. FITC-dextran is a water-soluble, membrane-impermeable, non-metabolised reagent that does not affect cellular activities (Klein & Satre, 1986; Oliver *et al*, 1984). It has no significant binding affinity for biological membranes and can be easily quantified by fluorescence. FITC-dextran was fully validated as a fluid-phase marker in *Dictyostelium* amoebae by the following observations: (1) FITC-dextran initial uptake rate varied linearly with extracellular FITC-dextran concentration (up to 20 mg/ml). (2) uptake was virtually abolished at 4°C. (3) FITC-dextran was not toxic to *Dictyostelium* amoebae as seen by the absence of inhibitory effect on growth. (4) FITC-dextran was not degraded by *Dictyostelium* as measured by the stability of its elution profile on a molecular sieve column after incubation with cells.

As shown in Fig.2, *Dictyostelium* amoebae suspended in nutritive medium that contained FITC-dextran progressively accumulated the fluorescent probe. The rate of accumulation was initially rapid but it decreased after 1.5-2 h and eventually reached a plateau. This plateau was not the result of cell exhaustion, since an identical pattern of fluid uptake was seen when another fluid-phase marker such as pyranine (Padh *et al*, 1993) was added after a 1.5 h-incubation in medium containing FITC-dextran (Fig. 2).

Given an average volume of 500-600 μm^3 for *Dictyostelium* amoebae of the axenic strain Ax-2 (Klein & Satre, 1986), the endocytic index at the plateau is $\geq$ 100% of the cell volume and thus cannot realistically give an estimate of the true physical volume of endocytic compartments. This observation indicates that internalised fluid-phase marker is

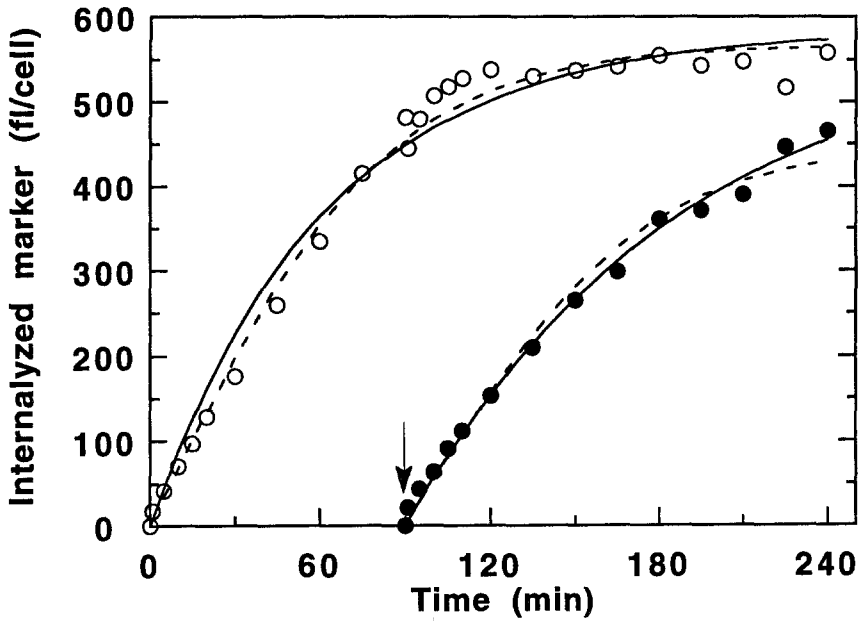

Fig. 2. Kinetics of FITC-dextran uptake in *Dictyostelium* amoebae. Cells (5×10^6 /ml) were incubated at 21°C in nutritive medium with 4 mg/ml FITC-dextran. At t = 1.5 hours, pyranine (0.2 mg/ml) was added as indicated by the arrow. Uptake of FITC-dextran (○) or pyranine (●) was determined as described under "Material and Methods" and expressed as fluid entry as a function of time. Uptake was fitted to a single compartment model and the solid lines drawn through the data points correspond to the following parameters: U_{max} = 585 fl/cell and λ = 0.016 min^{-1} (○) and U_{max} = 578 fl/cell and λ = 0.010 min^{-1} (●). The dashed lines correspond to a three-compartment fit (Blomhoff *et al*, 1989) with U_{max} = 566 fl/cell and uptake rate = 6.7 fl/cell/min (○) and U_{max} = 450 fl/cell and uptake rate = 5.3 fl/cell/min (●). Forward rate constants were λ_1 = 0.037 min^{-1}; λ_2 = 0.037 min^{-1}; λ_3 = 0.035 min^{-1}. The recycling rate constants λ_4 and λ_5 from compartments 1 and 2 to extracellular medium were found negligible (lower than 2×10^{-5} min^{-1}).

concentrated intracellularly during the endocytic process. In other cells such as hepatocytes, internalised fluid-phase marker is also markedly concentrated (Scharschmidt *et al*, 1986). The concentrative behaviour during fluid-phase endocytosis appears to be of general occurrence in eucaryotes and is a property increasing the efficiency of fluid-phase endocytosis (Thilo, 1985). Thus endocytosed volumes discussed in this work should be considered as apparent volumes that take into account both the physical volume of the compartments and the concentration factor of the fluid-phase probe in a given compartment.

Fluid-phase influx kinetics quite analogous to those obtained in *Dictyostelium* were described in other cell types such as L-cells, Swiss 3T3 fibroblasts or *Entamoeba histolytica* (Aley *et al*, 1984; Davies & Ross, 1978; Van Deurs *et al*, 1984). In contrast, in cells such as macrophages or hepatocytes, the rate of accumulation was initially rapid but it decreased to a smaller value (Besterman *et al*, 1981; Scharschmidt *et al*, 1986). The presence of a plateau was usually not presented but evidence for it would have required uptake measurements over longer time spans than reported.

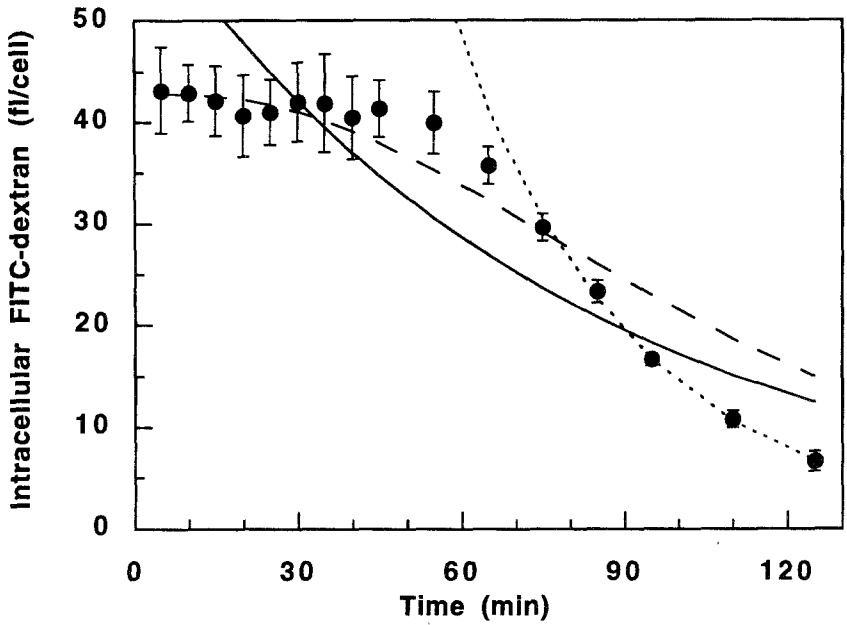

Fig. 3. Kinetics of FITC-dextran efflux. *Dictyostelium* amoebae (5×10^6 cells/ml) were incubated at 21°C in nutritive medium with 4 mg/ml FITC-dextran for 5 min. At the end of the pulse, cells were washed and chased at 21°C in nutritive medium without FITC-dextran. Intracellular FITC-dextran (●) was measured as a function of time. Three independent experiments were performed and data points shown in the graph are the average ± standard deviation from the mean. Lines drawn through the data points correspond to a one-compartment fit with $\lambda' = 0.013\ min^{-1}$ (continuous line ——); one-compartment fit on the last 5 points of the data with $\lambda' = 0.030\ min^{-1}$ (dotted line ····); and three-compartment fit (Blomhoff *et al*, 1989)(dashed line ----) with an uptake rate = 8.6 fl/cell/min and forward rate constants $\lambda_1 = 0.027\ min^{-1}$; $\lambda_2 = 0.028\ min^{-1}$; $\lambda_3 = 0.027\ min^{-1}$. The recycling rate constants λ_4 and λ_5 from compartments 1 and 2 to extracellular medium were found negligible (lower than $2 \times 10^{-6}\ min^{-1}$).

3.1.2 Pulse-Chase Experiments

To measure exocytosis, *Dictyostelium* amoebae were incubated for various pulse times in FITC-dextran-containing medium, washed at 0°C, reincubated in medium at 21°C for various chase periods, washed again and lysed. Fluorescence of the lysate represents cell-associated FITC-dextran. Efflux of FITC-dextran from *Dictyostelium* exhibited biphasic kinetics (Fig. 3). Upon return to 21°C in chase medium, there was a 30-40 min lag phase followed by a rapid release of the marker. The shorter the pulse, the longer the lag period and in cells where endocytic compartments were fully loaded with FITC-dextran, the lag time is almost absent (Aubry *et al*, 1993; Gonzalez *et al*, 1990; Padh *et al*, 1993). These fluid-phase marker efflux kinetics in *Dictyostelium* amoebae differ from those described in hepatocytes or macrophages where an immediate and rapid release was followed by a slower egress (Besterman *et al*, 1981; Scharschmidt *et al*, 1986).

3.2. Current Models of Fluid-Phase Endocytosis Kinetics

We first examined whether previous approaches described in the literature could be applied satisfactorily to *Dictyostelium* amoeba.

One-compartment model. The simplest fluid-phase endocytic kinetics are found in the parasitic amoeba *Entamoeba histolytica*. Evidence was given for an endocytic compartment in rapid equilibrium with the external milieu. Using the published data of Aley (Aley *et al*, 1984), we determined that the continuous influx of either FITC-dextran or horseradish peroxidase, another classical fluid-phase marker (Oliver *et al*, 1984), are satisfactorily described by a single compartment model. Data were fitted to the equation: $U(t) = U_{max}.(1-\exp(-\lambda t))$ and we found that in *Entamoeba histolytica* $U_{max} = 5600 \pm 900$ fl/cell and $\lambda = 0.017 \pm 0.004$ min^{-1} (mean ± s.d.; three experiments). Similarly, efflux of fluid-phase markers from fully loaded endocytic compartments was adjusted to the equation: $Q(t) = Q_{max}.\exp(-\lambda' t)$ with $\lambda' = 0.015-0.018$ min^{-1}.

An analogous approach was applied to *Dictyostelium* amoebae in two experimental conditions: i) continuous influx of fluid-phase marker, and ii) efflux from preloaded endocytic compartments (pulse-chase). A visually good fit was obtained between the experimental data points and the simulated curve for continuous FITC-dextran influx data (see Fig. 2). In contrast, efflux kinetics could not be adjusted to a one-compartment model as it is completely unable to account satisfactorily for the extended lag time in pulse-chase experiments. An increased complexity of the model was clearly needed in *Dictyostelium*. Nevertheless, the final part of the efflux kinetics corresponded to a first order process (Fig. 3).

Two- and three-compartment models. Several authors have previously proposed a multicompartmental analysis to describe fluid-phase marker influx and efflux data obtained from macrophages, fibroblasts, hepatocytes or reticulocytes (Besterman *et al*, 1981; Scharschmidt *et al*, 1986). In some models, two compartments were considered: one of small size and turning over very rapidly and a second one of larger apparent size, turning over quite slowly. The fluid-phase marker first enters the rapidly turning over compartment ($T_{1/2}$ = 1–8 min) identified collectively as the endosomes. From here, either it recycles to the extracellular space or it enters the slowly turning-over compartment ($T_{1/2}$ = 3–10h) identified as the lysosomes. No recycling of fluid was supposed to occur from lysosomes which were considered as dead-end spaces. *Dictyostelium* efflux kinetics could not be fitted by two-compartment models (not shown).

Another model was developed to analyse fluid-phase endocytosis in rabbit hepatocytes (Blomhoff *et al*, 1989). It considered three successive and kinetically distinct compartments identified to early endosomes, prelysosomes and lysosomes, respectively. An important feature of the model is that the best fit to experimental data in hepatocytes was obtained when all three compartments, thus including lysosomes, recycled material directly to the extracellular medium rather than to other intracellular compartments. This three-compartment description was used in a recent work on receptor-mediated endocytosis of transferrin to account simultaneously for fluid-phase endocytic activity in hepatocytes and reticulocytes (Bakøy & Thorstensen, 1994).

We applied the three-compartment model (Blomhoff *et al*, 1989), to fit FITC-dextran influx or efflux (chase) data obtained from *Dictyostelium* amoebae loaded by a short pulse (see Fig. 2 and 3). Continuous uptake was correctly described but pulse-chase data were not fitted by the three-compartment model and a more complicated model was needed.

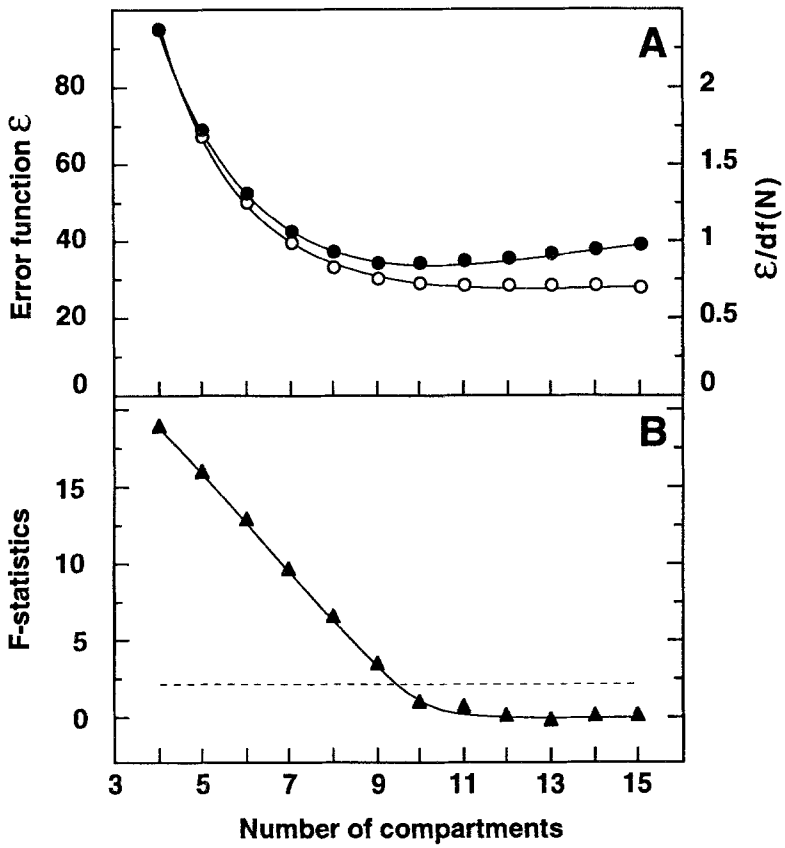

Fig. 4. Estimation of the minimal number of compartments required for modelling of fluid-phase pinocytosis kinetics. *Dictyostelium* amoebae (5×10^6 cells/ml) were incubated at 21°C in nutritive medium with 4 mg/ml FITC-dextran for a 5 min-pulse or continuously. Intracellular FITC-dextran was measured as a function of time and the two sets of data were fitted simultaneously to the multicompartmental model. The error functions: ε (○) or ε/*df*(*N*) (●) in panel A and the *F* statistics parameter (▲) in panel B (see Eqs. 5, 7 and 8 under "Material and Methods") are plotted as a function of the number of compartments. The dashed line in panel B correspond to the 90% confidence limit. The number of independent data available in both experimental series was 15. The *F* statistics was computed for $N2=N$ and $N1= N-1$.

3.3. Multicompartmental Model of Fluid-Phase Endocytosis in *Dictyostelium Discoideum*

The simplest way to increase the complexity of fluid-phase endocytosis models was to increase the number of compartments. The error function ε as defined in Eq. 5 (see "Material and Methods") was determined for increasing values of N on sets of data points corresponding to continuous uptake as well as 5 min pulse-chase experiments (Fig. 4A). We observed that ε decreased substantially when N increased but without any pronounced minimum. The derived plot of the error per degree of freedom: $\varepsilon(N)/df(N)$ as a function of N shows a shallow minimum around N = 9-10. Furthermore, F test (Landaw &

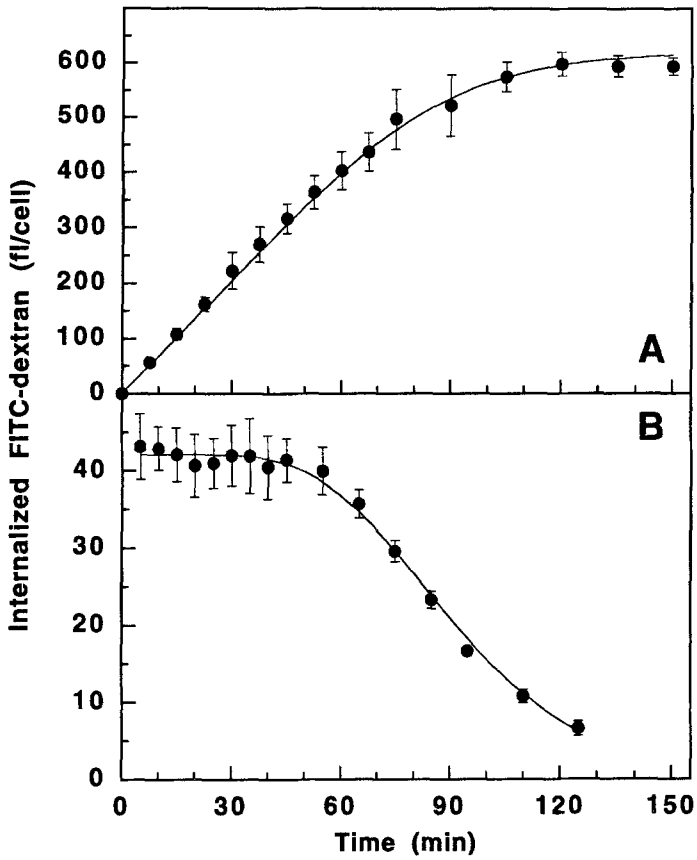

Fig. 5. Multicompartmental modelling of fluid-phase endocytosis kinetics in *Dictyostelium* amoebae. Data were obtained either from three independent continuous loading- (Panel A) or 5 min-pulse experiments (Panel B; data taken from Fig. 3). All points shown in the figure are the average ± standard deviation from the mean. Before calculations, each temporal set was normalised individually. The mean values and variances were then determined for homologous data (i.e. charge or 5 min-pulse). Finally, these sets of data were treated simultaneously according to Eq. 5. Continuous lines drawn through data points correspond to the best fits to the multicompartmental model with $N = 9$. The successive λ_i (in min^{-1} ; $i = 1$ to 9) were the following: 0.090; 0.127; 0.099; 0.090; 0.093; 0.098; 0.098; 0.111; 0.096. The fluid influx rate μ was calculated to be 6.8 and 8.4 fl/cell/min for continuous uptake and pulse chase experiments, respectively. The apparent volume of the endocytic pathway $U_{max} = (U_1 + U_2 + ... + U_9)$ was 646 fl/cell.

DiStefano, 1984) as shown in Fig. 4B demonstrates that the improvement achieved by increasing N from 9 to 10 was not statistically significant ($p = 0.1$).

In Fig.5 are shown the best fits obtained with the 9-compartment model applied to continuous uptake and to 5-min pulse experiments. The model clearly accounted correctly for continuous uptake as expected already from the results shown in Fig. 2 but the adequacy of the fit is fully appreciated on pulse-chase data. The 9-compartment model gives a nice fit for the long latency period before FITC-dextran efflux in the pulse-chase experiment (see

Fig. 5B). Similar values were found for the successive rate constants λ_i that vary within less than a 15% range. This suggests that all compartments considered in the model have grossly similar apparent volumic contributions to the endocytic pathway.

The number of compartments needed to obtain a satisfactory model of fluid-phase endocytosis in *Dictyostelium* amoebae is higher than the number of biochemically distinguished compartments in the endocytic pathway, i.e. coated vesicles, early endosomes, late endosomes, secondary lysosomes, postlysosomal recycling vesicles (Aubry *et al*, 1993; Courtoy, 1991; Padh *et al*, 1993). This observation would rather favour a maturation model of endocytosis (Murphy, 1991) where the high value of N in the mathematical model would reflect the gradual evolution of the compartments during vesicular progression. Alternatively, the vesicular shuttle hypothesis (Griffiths & Gruenberg, 1991) between a limited number of preexisting compartments and supported in *Dictyostelium* by in vitro fusion experiments (Lenhard *et al*, 1992) would definitely require the incorporation of some form of maturation steps. Along these lines and by including endo-lysosomal acidification kinetics (Aubry *et al*, 1993) as additional experimental data, we hope to further refine the mathematical modelling of fluid-phase endocytosis in *Dictyostelium* amoebae.

ACKNOWLEDGEMENTS

We are most grateful to Ms. Mireille Bof for her excellent technical assistance and Ms. Maribel Chenin for maintenance of the computation facilities. This work was supported by grants from the Centre National de la Recherche Scientifique (Unités de Recherche Associées 1130 and 1618) and the Commissariat à l'Énergie Atomique.

REFERENCES

Aley, S., Z. Cohn and W. Scott (1984). Endocytosis in *Entamoeba histolytica*. Evidence for a unique non-acidified compartment. Journal of Experimental Medicine 160: 724-737.

Atkins, G.L. (1973). Modèles à Compartiments Multiples pour les Systèmes Biologiques, pp. 1-181. Paris-Bruxelles-Montréal, Gauthier-Villars.

Aubry, L., G. Klein, J.L. Martiel and M. Satre (1993). Kinetics of endosomal pH evolution in *Dictyostelium discoideum* amoebae. Study by fluorescence spectroscopy. Journal of Cell Science 105: 861-6.

Bakøy, O.E. and K. Thorstensen (1994). The process of cellular uptake of iron from transferrin. A computer simulation program. European Journal of Biochemistry 222: 105-112.

Berlin, R. and J. Oliver (1980). Surface functions during mitosis. II. Quantification of pinocytosis and kinetic characterization of the mitotic cycle with a new fluorescence technique. Journal of Cell Biology 85: 660-671.

Berlin, R.D., J.M. Oliver and R.J. Walter (1978). Surface functions during mitosis. I: Phagocytosis, pinocytosis and mobility of surface-bound ConA. Cell 15: 327-341.

Besterman, J. and R. Low (1983). Endocytosis : a review of mechanisms and plasma membrane dynamics. Biochemical Journal 210: 1-13.

Besterman, J.M., J.A. Airhart, R.C. Woodworth and R.B. Low (1981). Exocytosis of pinocytosed fluid in cultured cells: kinetic evidence for rapid turnover and compartmentation. Journal of Cell Biology 91: 716-727.

Blomhoff, R., M.S. Nenseter, M.H. Green and T. Berg (1989). A multicompartmental model of fluid-phase endocytosis in rabbit liver parenchymal cells. Biochemical Journal 262: 605-610.

Clarke, M. and S.C. Kayman (1987). The axenic mutations and endocytosis in *Dictyostelium*. Methods in Cell Biology 28: 157-176.

Courtoy, P.J. (1991). Dissection of endosomes. In: C. Steer and J. Hanover, ed., Intracellular Trafficking of Proteins, pp. 103-156. Cambridge, Cambridge University Press.

Davies, P.F. and R. Ross (1978). Mediation of pinocytosis in cultured arterial smooth muscle and endothelial cells by platelet-derived growth factor. Journal of Cell Biology 79: 663-671.

De Belder, A.N. and K. Granath (1973). Preparation and properties of fluorescein labelled dextrans. Carbohydrate Research 30: 375-378.

DiStefano, J.J.I. and E.M. Landaw (1984). Multiexponential, multicompartmental, and noncompartmental modeling. I. Methodological limitations and physiological interpretations. American Journal of Physiology 246: R651-R664.

Gonzalez, C., G. Klein and M. Satre (1990). Caffeine, an inhibitor of endocytosis in *Dictyostelium discoideum* amoebae. Journal of Cellular Physiology 144: 408-415.

Griffiths, G. and J. Gruenberg (1991). The arguments for pre-existing early and late endosomes. Trends in Cell Biology 1: 5-10.

Helenius, A., I. Mellman, D. Wall and A. Hubbard (1983). Endosomes. Trends in Biochemical Sciences 8: 245-250.

IMSL (1991). International Mathematical and Statistical Library (IMSL) user's manual: Fortran routines for mathematical applications and statistical analysis. Version 2.0. Visual Numerics, Inc., Customer Relations, 9990 Richmond, Suite 4000, Houston, TX 77042 (USA).

Keen, J.H. (1990). Clathrin and associated assembly and disassembly proteins. Annual Review of Biochemistry 59: 415-438.

Klein, G. and M. Satre (1986). Kinetics of fluid-phase pinocytosis in *Dictyostelium discoideum* amoebae. Biochemical and Biophysical Research Communications 138: 1146-1152.

Landaw, E.M. and J.J.I. DiStefano (1984). Multiexponential, multicompartmental, and noncompartmental modeling. II. Data analysis and statistical considerations. American Journal of Physiology 246: R665-R677.

Lenhard, J.M., L. Mayorga and P.D. Stahl (1992). Characterization of endosome-endosome fusion in a cell-free system using *Dictyostelium discoideum*. Journal of Biological Chemistry 267: 1896-1903.

Loomis, W.F.J. (1971). Sensitivity of *Dictyostelium discoideum* to nucleic acid analogues. Experimental Cell Research 64: 484-486.

Maeda, Y. (1983). Axenic growth of *Dictyostelium discoideum* wild type NC-4 cells and its relation to endocytic ability. Journal of General Microbiology 129: 2467-2474.

Murphy, R.F. (1991). Maturation models for endosome and lysosome biogenesis. Trends in Cell Biology 1: 77-82.

O'Halloran, T.J. and R.G. Anderson (1992). Characterization of the clathrin heavy chain from *Dictyostelium discoideum*. DNA and Cell Biology 11: 321-330.

O'Halloran, T.J. and R.G. Anderson (1992). Clathrin heavy chain is required for pinocytosis, the presence of large vacuoles, and development in *Dictyostelium*. Journal of Cell Biology 118: 1371-1377.

Oliver, J.M., R.D. Berlin and B.H. Davis (1984). Use of horseradish peroxidase and fluorescent dextrans to study fluid pinocytosis in leukocytes. Methods in Enzymology 108: 336-347.

Padh, H., J. Ha, M. Lavasa and T.L. Steck (1993). A post-lysosomal compartment in *Dictyostelium discoideum*. Journal of Biological Chemistry 268: 6742-6747.

Quintart, J., M.A. Leroy-Houyet, A. Trouet and P. Baudhuin (1979). Endocytosis and chloroquine accumulation during the cell cycle of hepatoma cells in culture. Journal of Cell Biology 82: 644-653.

Ruscetti, T., J.A. Cardelli, M.L. Niswonger and T.J. O'Halloran (1994). Clathrin heavy chain functions in sorting and secretion of lysosomal enzymes in *Dictyostelium discoideum*. Journal of Cell Biology 126: 343-352.

Sandvig, K. and B. Van Deurs (1991). Endocytosis without clathrin (a minireview). Cell Biology International Report 15: 3-8.

Scharschmidt, B.F., J.R. Lake, E.L. Renner, V. Licko and R.W. Van Dyke (1986). Fluid phase endocytosis by cultured rat hepatocytes and perfused rat liver: Implications for plasma membrane turnover and vesicular trafficking of fluid phase markers. Proceedings of the National Academy of Science of the United States of America 83: 9488-9492.

Smythe, E. and G. Warren (1991). The mechanism of receptor-mediated endocytosis. European Journal of Biochemistry 202: 689-699.

Sorkin, A. and C.M. Waters (1993). Endocytosis of growth factor receptors. BioEssays 15: 375-82.

Steinman, R., I. Mellman, W. Muller and Z. Cohn (1983). Endocytosis and the recycling of plasma membrane. Journal of Cell Biology 96: 1-27.

Swanson, J.A., D.L. Taylor and J.T. Bonner (1981). Coated vesicles in *Dictyostelium discoideum*. Journal of Ultrastructure Research 75: 243-249.

Swanson, J.A., B.D. Yirinec and S.C. Silverstein (1985). Phorbol esters and horseradish peroxidase stimulate pinocytosis and redirect the flow of pinocytosed fluid in macrophages. Journal of Cell Biology 100: 851-859.

Thilo, L. (1985). Quantification of endocytosis-derived membrane traffic. Biochimica et Biophysica Acta 822: 243-266.

Van Deurs, B., O. Petersen, S. Olsnes and K. Sandvig (1989). The ways of endocytosis. International Review of Cytology 117: 131-177.

Van Deurs, B., C. Röpke and N. Thorball (1984). Kinetics of pinocytosis studied by flow cytometry. European Journal of Cell Biology 34: 96-102.

Watts, C. and M. Marsh (1992). Endocytosis: what goes in and how? Journal of Cell Science 103: 1-8.

Watts, D.J. and J.M. Ashworth (1970). Growth of myxamoebae of the cellular slime mould *Dictyostelium discoideum* in axenic culture. Biochemical Journal 119: 171-174.